

UNCLASSIFIED

AD 435976

DEFENSE DOCUMENTATION CENTER

FOR

SCIENTIFIC AND TECHNICAL INFORMATION

CAMERON STATION, ALEXANDRIA, VIRGINIA



UNCLASSIFIED

NOTICE: When government or other drawings, specifications or other data are used for any purpose other than in connection with a definitely related government procurement operation, the U. S. Government thereby incurs no responsibility, nor any obligation whatsoever; and the fact that the Government may have formulated, furnished, or in any way supplied the said drawings, specifications, or other data is not to be regarded by implication or otherwise as in any manner licensing the holder or any other person or corporation, or conveying any rights or permission to manufacture, use or sell any patented invention that may in any way be related thereto.

64-12

REPORT NO.
ATN-64(9236)-14

435976

4359.6

CATALOGED BY DDC
AS AD No. _____

General Research

Mechanical Behavior of Sapphire

23 MARCH 1964

*Prepared by H. CONRAD
Materials Sciences Laboratory*

*Prepared for VICE PRESIDENT and GENERAL MANAGER
LABORATORY OPERATIONS*

APR 22 1964
ADD 22 1964
TICIA A


AEROSPACE CORPORATION

Report No.
ATN-64(9236)-14

GENERAL RESEARCH
Mechanical Behavior of Sapphire

Prepared by
H. Conrad
Materials Sciences Laboratory

AEROSPACE CORPORATION
El Segundo, California

23 March 1964

Prepared for
VICE PRESIDENT AND GENERAL MANAGER
LABORATORY OPERATIONS

APPROVAL OF REPORT CONTENT

(Attach to front cover of draft; return to Publications Section after final approval. This page is not to appear in the report.)

Title: General Research:
Mechanical Behavior
of Sapphire

Report No. ATN-64(9236)-14

Classification: Unclassified

PWO: 74-2416

Date: 23 March 1964

Author: H. Conrad

Approval:



J. E. Hove, Director
Materials Sciences Laboratory

ABSTRACT

The present state of our knowledge on the mechanical behavior of sapphire is reviewed: Sapphire deforms plastically at temperatures above 900°C, the most common mode of deformation being slip on the basal plane in the $\langle 11\bar{2}0 \rangle$ direction. However, under certain conditions, slip may occur on prism planes or twinning may occur. A yield point is often observed. This appears to be related to the multiplication of dislocations by a mechanism which is controlled by the motion of dislocations through the lattice, rather than by the tearing of dislocations from an impurity (or defect) atmosphere. The dynamics of yielding and flow is similar and can be expressed by either of two thermally activated equations. In one, the effect of stress is principally on the pre-exponential frequency factor; in the other, its effect is principally on the activation energy. There is insufficient data to permit a positive decision between the two, or to positively identify the rate-controlling dislocation mechanism. Fracture generally occurs on a plane approximately normal to the tensile stress, and the fracture surface is conchoidal. In the temperature range from 1100° to 1500°C, the tensile fracture stress decreases with increase in plastic strain, independent of temperature and strain rate. The mechanism of failure in this case seems to be the interaction of edge dislocations with pre-existing cracks.

CONTENTS

I. INTRODUCTION 1

II. PLASTIC FLOW BY SLIP 1

 A. Geometry of Slip 1

 B. Dislocation Structure 3

 C. Dynamics of Slip 7

 D. The Yield Point 18

III. TWINNING 19

IV. FRACTURE 22

V. SUMMARY 29

REFERENCES 32

TABLE

1. The Values of the Constants A, n, and H in the
Equation $\dot{\gamma} = (A/T)[(\tau^*)^n \exp-(H/RT)]$ Derived from
Data in the Literature 14

FIGURES

| | | |
|-----|--|----|
| 1. | Arrangement of Aluminum Ions and Holes Between Two Layers of Oxide Ions. Large open circles represent underlying oxide ions, small open circles represent holes and small filled circles represent aluminum ions. The upper layer of oxide ions is not shown. Basal hexagonal cell vectors and directions are shown. [After Kronberg (Ref. 1)] | 2 |
| 2. | Schematic of the Two Experimentally Observed Slip Systems in Sapphire. [After Scheuplein and Gibbs (Ref. 6)] | 4 |
| 3. | Dislocation Etch Pits in Basally Bent Sapphire Rod Density = $3.2 \times 10^7 \text{ cm}^{-2}$ (orig. mag. 1800 X). [After Scheuplein and Gibbs (Ref. 6)] | 5 |
| 4. | Dislocation Structure on the (0001) Surface of a 0 deg Ruby Crystal (orig. mag 30 X). [After Janowski and Conrad (Ref. 12)] | 6 |
| 5. | Dislocations in Sapphire Lying Along the $\langle 11\bar{2}0 \rangle$ Directions (orig. mag. 1000 X). [After Bond and Harvey (Ref. 14)] | 8 |
| 6. | Hexagonal Arrays of Dislocations in the Basal Plane of Sapphire (orig. mag. 20,000 X). [After Voruz, Jewett, and Accountius (Ref. 15)] | 9 |
| 7. | Effect of Temperature and Strain Rate on the Upper and Lower Yield Stresses of Sapphire. (a) Effect of Temperature for a Constant Crosshead Velocity of 2×10^{-4} in./min. (b) Effect of Strain Rate at a Constant Temperature of 1420°C. [After Kronberg (Ref. 8)] | 10 |
| 8. | Effect of Temperature on the Upper and Lower Yield Stresses of Sapphire. (a) Upper Yield Stress; (b) Lower Yield Stress. [After Kronberg (Ref. 8)] | 11 |
| 9. | Effect of Temperature and Strain Rate on the Flow Stress of Sapphire in Tension. Also Shown are the Values of $n = (\partial \ln \dot{\gamma}) / (\partial \ln \tau_o)$. [After Conrad (Ref. 7)] | 12 |
| 10. | Activation Energy for Plastic Flow of Sapphire as a Function of Temperature Assuming an Equation of the Form $\dot{\gamma} = A(\tau^*)^n \exp(-H_o/RT)$ | 16 |
| 11. | Activation Energy for Plastic Flow of Sapphire as a Function of Temperature Assuming an Equation of the Form $\dot{\gamma} = v \exp[-H(\tau^*)/RT]$ | 17 |

FIGURES (Continued)

| | | |
|-----|---|----|
| 12. | Twin Bands in Sapphire Compression Specimens [After Stofel and Conrad (Ref. 31)] | 20 |
| 13. | Effect of Temperature on the Upper Yield Load in Compression and on Twinning. [After Conrad, Stone and Janowski (Ref. 17)] | 21 |
| 14. | Effect of Temperature on the Modulus of Rupture of Sapphire and Ruby. [After Wachtman and Maxwell (Ref. 32)] | 23 |
| 15. | Variation of the Fracture Stress in Tension with Strain at Fracture [After Stofel and Conrad (Ref. 31)] | 24 |
| 16. | (a) Typical Fracture Surface Produced During Tensile Testing of a 60 deg Sapphire Rod. Fracture Origin is at Bottom. (b) Enlarged View of Transition from Mirror Area to Wallner Lines on Fracture Surface of Above Figure. [After Stofel and Conrad (Ref. 31)] | 25 |
| 17. | Orowan's Model of Crack Growth Induced by Plastic Flow. Crack Front Moves from a to c as Plastic Strain Increases. [After Stofel and Conrad (Ref. 31)] | 26 |
| 18. | Reciprocal of Fracture Tensile Stress Squared as a Function of Shear Strain. [After Stofel and Conrad (31)] | 28 |

I. INTRODUCTION

An understanding of the mechanical behavior of aluminum oxide is of importance from a technological, as well as a scientific, standpoint. Because of its stability, inertness, and high melting point ($\sim 2050^\circ\text{C}$), aluminum oxide offers some promise as a structural material for use in air at high temperatures. Furthermore, cracking (brittleness) is a problem in the growth and use of sapphire and ruby for such applications as bearings and lasers.

The present paper critically reviews the present state of our knowledge on the mechanical behavior (slip, twinning, and fracture) of sapphire.

II. PLASTIC FLOW BY SLIP

A. GEOMETRY OF SLIP

The crystal structure of sapphire consists of oxygen ions very nearly in hexagonal closest packing with aluminum ions tucked into the octahedral interstices of the oxygen framework. The atomic arrangement looking down on the basal plane is shown in Fig. 1.

Nye (Ref. 2), Wachtman and Maxwell (Refs. 3, 4), Kronberg (Refs. 1, 5, 8), Scheuplein and Gibbs (Ref. 6), and Conrad (Ref. 7), have established rather conclusively that, in the temperature range from 1000° to 2000°C , sapphire deforms plastically in tension, compression, and bending by slip on the basal plane in the $\langle 11\bar{2}0 \rangle$ direction, i. e., in the direction of the closest packing of the interstitial holes rather than in the closest packing of the oxygen atoms. Under certain conditions, slip has also been observed to occur on the second-order prism planes. For example, Wachtman and Maxwell (Refs. 9, 10) found creep to occur on a "second unidentified system" above 1600°C , while Klassen-Neklyudova (Ref. 11) reported slip on $[1\bar{2}10]$

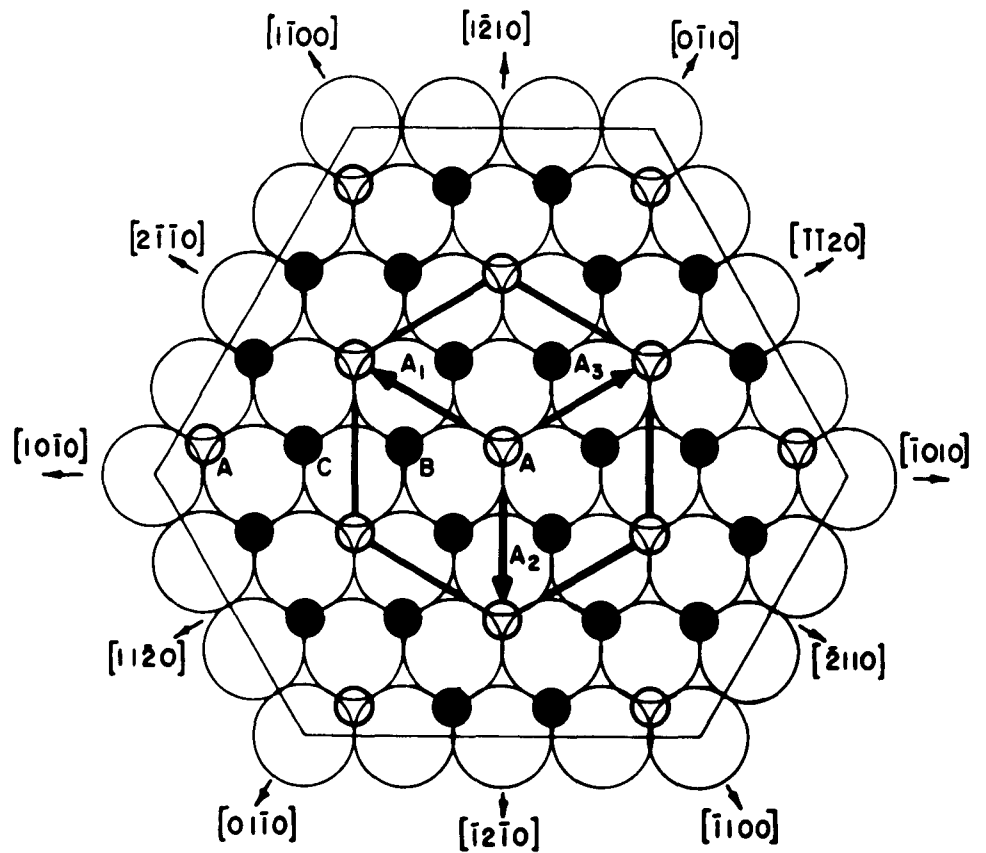


Fig. 1. Arrangement of Aluminum Ions and Holes Between Two Layers of Oxide Ions. Large open circles represent underlying oxide ions, small open circles represent holes and small filled circles represent aluminum ions. The upper layer of oxide ions is not shown. Basal hexagonal cell vectors and directions are shown. [After Kronberg (Ref. 1)]

planes in $\langle 10\bar{1}0 \rangle$ directions (i. e. , on the prismatic slip system) above 2000°C . Scheuplein and Gibbs (Ref. 6) also observed prismatic slip for special conditions of deformation at temperatures from 1800° to 2000°C . The two observed slip systems are depicted schematically in Fig. 2.

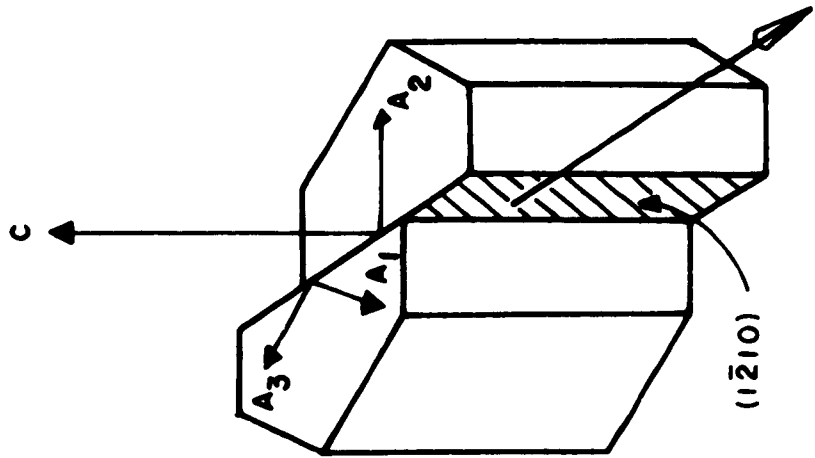
B. DISLOCATION STRUCTURE

It is now generally recognized that slip in crystalline solids occurs by the motion of the crystal defect termed a dislocation. Kronberg (Ref. 1) was the first to consider the atomic arrangements about a dislocation in sapphire and suggested that the basal dislocation in sapphire might actually consist of four partials. Subsequently, Scheuplein and Gibbs (Ref. 6) revealed dislocations in sapphire by the etch-pit technique, using boiling phosphoric acid as the reagent. They reported that the density of basal dislocations in annealed as-grown crystals was 1 to $3 \times 10^{-6}\text{cm}^{-2}$, while that of the prismatic dislocations was about 10^5cm^{-2} . These values increased to 1 to $3 \times 10^7\text{cm}^{-2}$ after straining by bending. An example of the dislocation etch pits observed by them in a basally bent sapphire rod is shown in Fig. 3.

Alford and Stephens (Ref. 11) later established that dislocations in sapphire and ruby could also be revealed by etching in fused potassium bisulfate (KHSO_4) at 675°C . Janowski and Conrad (Ref. 12) used this etch to map the dislocation structure of sapphire and ruby crystals; see, for example, Fig. 4. These latter authors found that the average dislocation density on the basal plane of ruby was 1.5 to $3 \times 10^6\text{cm}^{-2}$, while that on the prismatic $[11\bar{2}0]$ plane was $5 \times 10^5\text{cm}^{-2}$, indicating a lower density of basal dislocations as compared with prismatic dislocations, in contrast to the observations of Scheuplein and Gibbs (Ref. 6) for sapphire.

The termini of basal dislocations on the $\{11\bar{2}0\}$ and on the $\{10\bar{1}0\}$ planes of sapphire have been revealed by Palmour and Kriegel (Ref. 13) by thermal etching. Furthermore, Emond and Harvey (Ref. 14) were able to decorate dislocations in sapphire by adding 1 percent by weight ZrO_2 to

PRISMATIC SLIP



BASAL SLIP

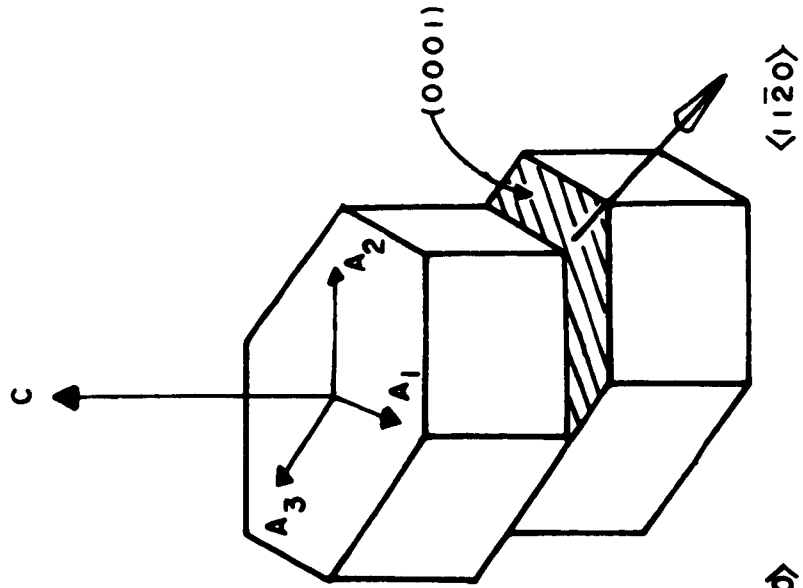


Fig. 2. Schematic of the Two Experimentally Observed Slip Systems in Sapphire.
[After Scheuplein and Gibbs (Ref. 6)]

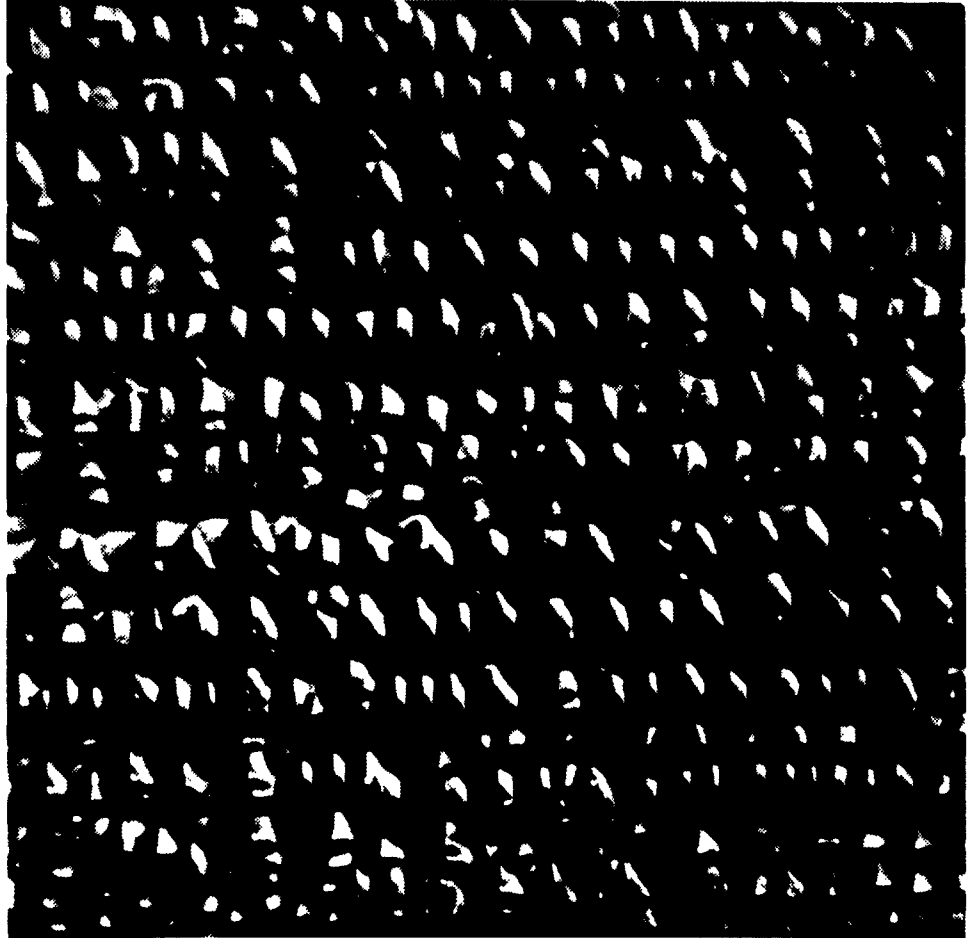


Fig. 3. Dislocation Etch Pits in Basally Bent Sapphire Rod
Density = $3.2 \times 10^7 \text{ cm}^{-2}$ (orig. mag. 1800 \times). [After
Scheuplein and Gibbs (Ref. 6)]

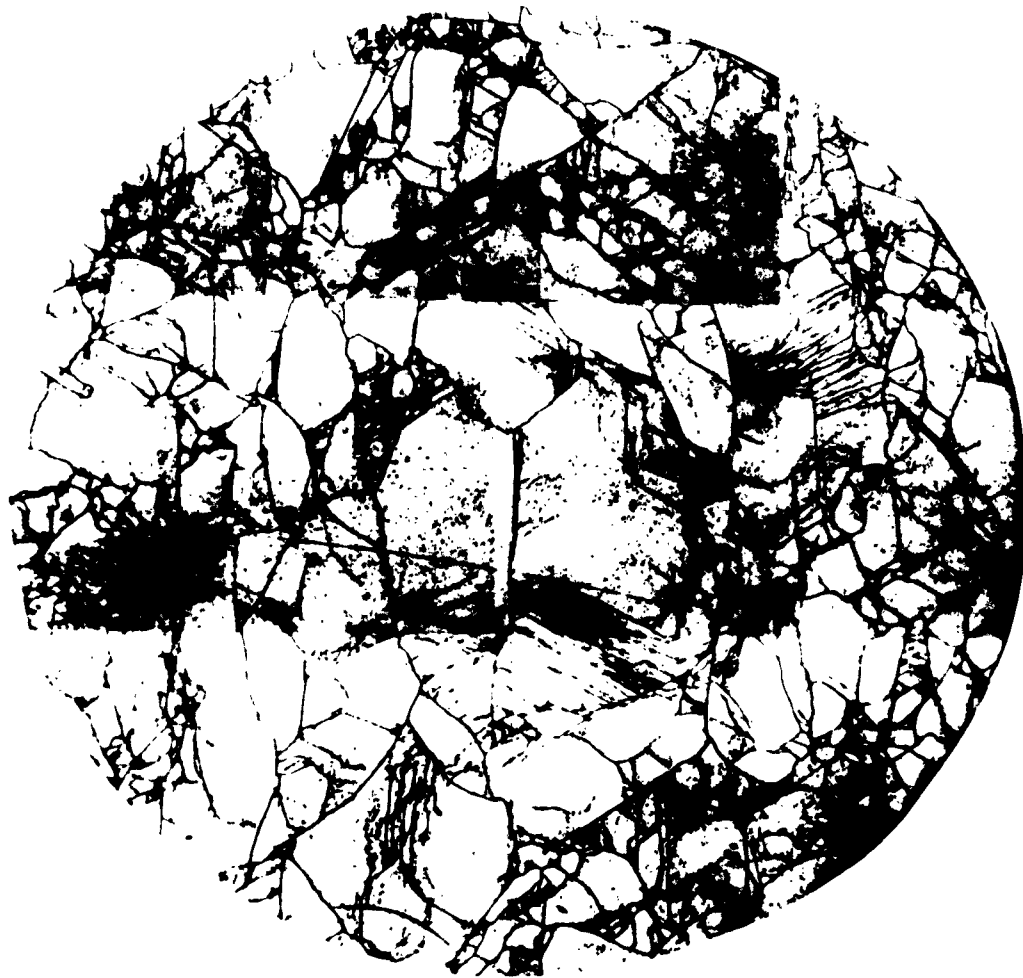


Fig. 4. Dislocation Structure on the (0001) Surface of a 0 deg Ruby Crystal (orig. mag. 30 ×). [After Janowski and Conrad (Ref. 12)]

the Al_2O_3 powder used in the growth of crystals by the Verneuil technique and then heating the crystals for four hours at 1500°C . Examination of the crystals by optical transmission microscopy revealed that many dislocations had straight segments that were parallel to one of the six $\langle 11\bar{2}0 \rangle$ directions in the basal plane; see Fig. 5. Subsequently, direct observations of dislocations in sapphire platelets by electron transmission was made by Veruz, Jewett, and Accountis (Ref. 15), Fig. 6. They suggested that the apparent double images seen in Fig. 6 represent partial dislocations separated by ribbons of fault, in support of Kronberg's (Ref. 1) suggestion that the dislocations in sapphire may be split into partials. However, Wachtman (Ref. 16), reporting on electron transmission studies underway at the National Bureau of Standards, stated that such double images were not observed for dislocations in specimens thinned from the bulk and, further, that there was no evidence of quarter partials in their specimens.

C. DYNAMICS OF SLIP

Wachtman and Maxwell (Refs. 3, 4) first reported that the creep behavior of sapphire at temperatures from 1000° to 1300°C was similar to that of metals that exhibit a yield point; i. e., creep occurred suddenly at a well defined stress, and the creep curve was S-shape in character. Subsequently, Kronberg (Ref. 8) and Conrad (Ref. 7) established that a yield point does actually occur during the tensile and compressive straining in the temperature range from 1100° to 1700°C . Examples of the stress-strain curves observed by Kronberg (Ref. 8) are shown in Fig. 7. It is here seen that the upper and lower yield stresses and the amount of the yield drop increases with increase in strain rate and decrease in temperature. The effect of strain rate and temperature on the upper and lower yield stresses is shown in Fig. 8. Similar results were obtained by Conrad (Ref. 7) and Conrad, et al (Ref. 17), for tension and compression tests.

The effect of strain rate and temperature on the flow stress subsequent to the lower yield stress was investigated by Conrad and coworkers (Refs. 7, 17), using "differential" type tests (i. e., those in which the temperature or strain rate are changed during the test), as depicted in Fig. 9. The effect

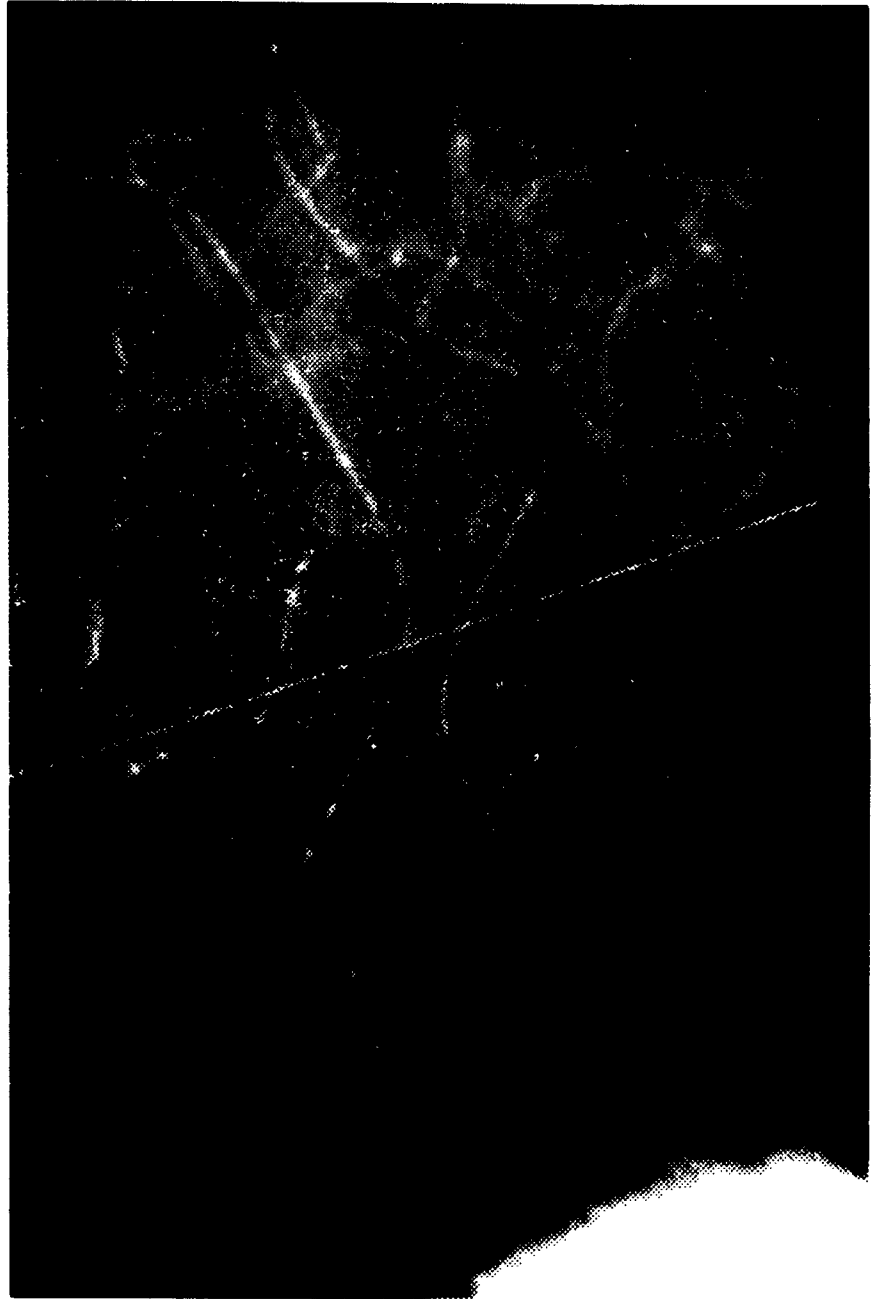


Fig. 5. Dislocations in Sapphire Lying Along the $\langle 11\bar{2}0 \rangle$ Directions (orig. mag. 1000 X).
[After Bond and Harvey (Ref. 14)]



Fig. 6. Hexagonal Arrays of Dislocations in the Basal Plane of Sapphire (orig. mag. 20,000 X). [After Voruz, Jewett, and Accountius (Ref. 15)]

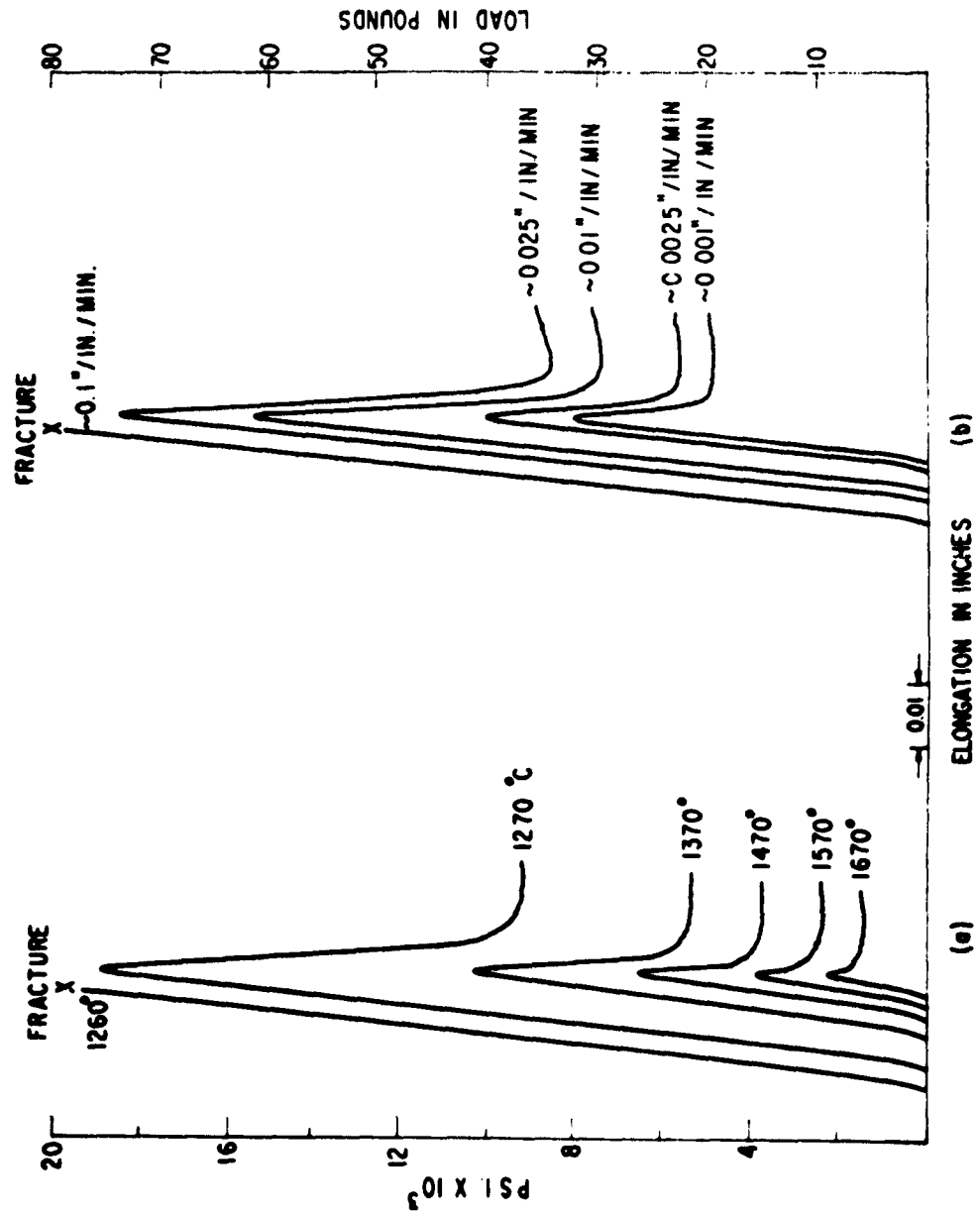


Fig. 7. Effect of Temperature and Strain Rate on the Upper and Lower Yield Stresses of Sapphire. (a) Effect of Temperature for a Constant Crosshead Velocity of 2×10^{-4} in./min. (b) Effect of Strain Rate at a Constant Temperature of 1420°C . [After Kronberg (Ref. 8)]

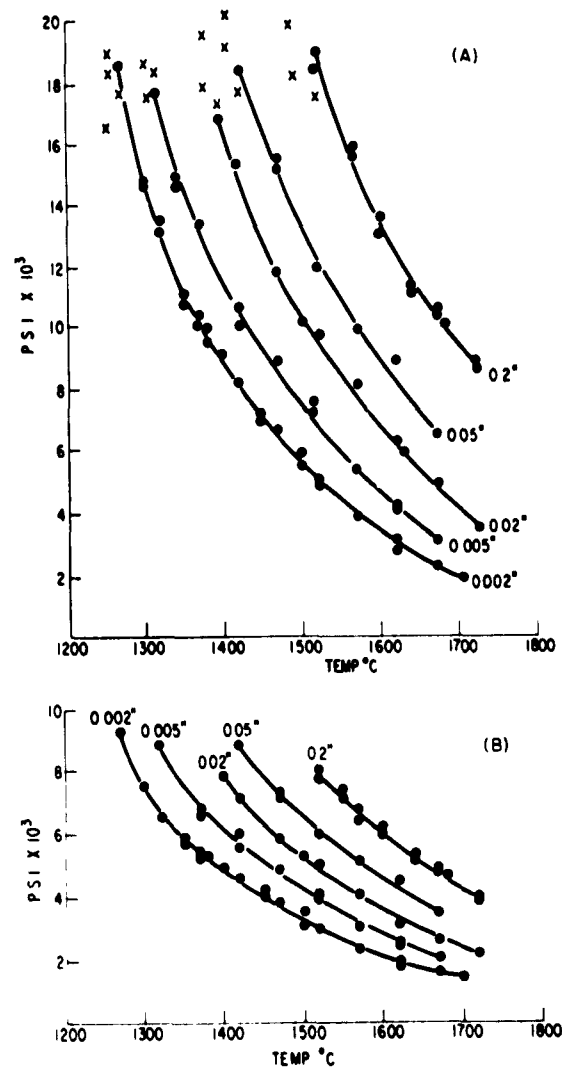


Fig. 8. Effect of Temperature on the Upper and Lower Yield Stresses of Sapphire. (a) Upper Yield Stress; (b) Lower Yield Stress. [After Kronberg (Ref. 8)]

VERTICAL ARROWS INDICATE WHERE CHANGES IN STRAIN RATE WERE MADE

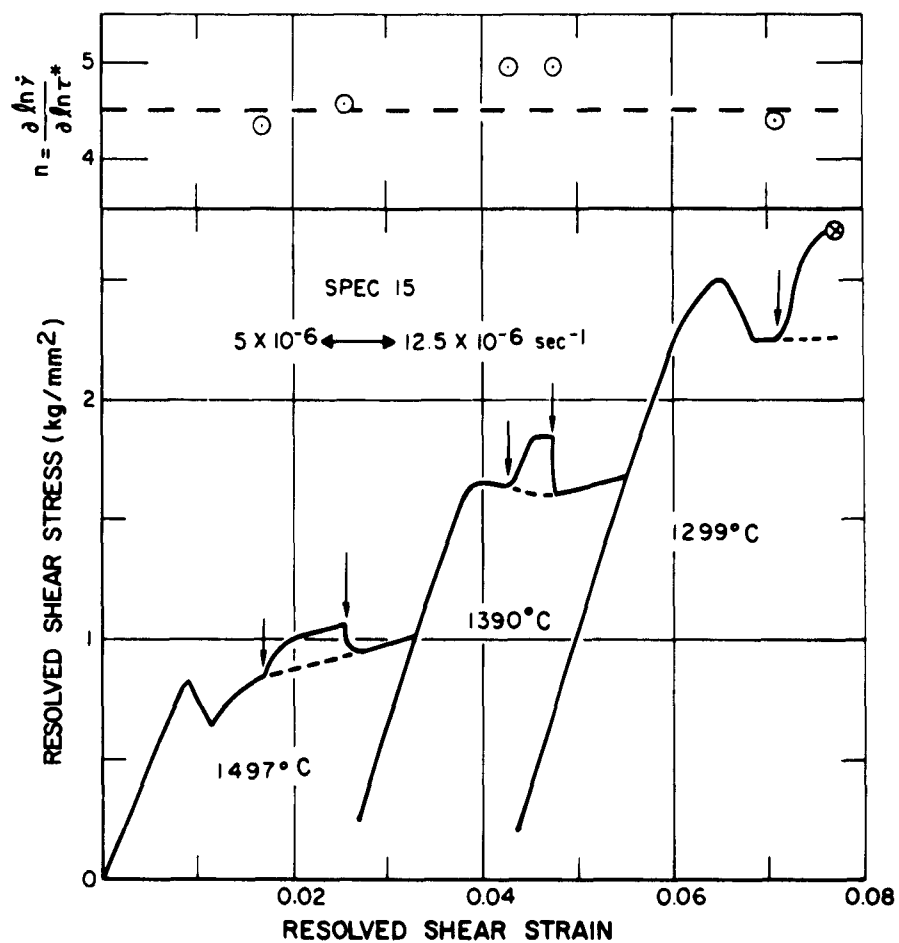


Fig. 9. Effect of Temperature and Strain Rate on the Flow Stress of Sapphire in Tension. Also Shown are the Values of $n = (\partial \ln \dot{\gamma}) / (\partial \ln \tau_0)$. [After Conrad (Ref. 7)]

of temperature and stress on the creep rate of sapphire was studied by Rogers, Baker, and Gibbs (Ref. 18) in the temperature range from 1000° to 1200° and of sapphire and ruby by Chang (Ref. 19) at 1500° to 1900°C. An analysis of the available data on the yielding and flow of sapphire indicates that the dynamics of yielding (proportional limit, upper yield stress and lower yield stress), and flow (flow stress, creep) is similar and can be expressed as either

$$\dot{\gamma} = \frac{A}{T} (\tau^*)^n \exp\left(-\frac{H_0}{RT}\right) \quad (1)$$

or

$$\dot{\gamma} = \nu \exp\left[-\frac{H(\tau^*)}{RT}\right] \quad (2)$$

where $\dot{\gamma}$ is the resolved shear strain rate, A , n , and ν are constants for a given yielding or flow stress, τ^* is the effective resolved shear stress; for flow τ^* is given approximately by the critical resolved lower yield stress at a given temperature and strain rate. † H_0 and $H(\tau^*)$ are the activation energies, being independent of stress in one case and decreasing with the stress in the other.

The values of the constants derived from data in the literature using Eq. (1) are given in Table 1. The scatter in the data and the lack of data over a very wide temperature range preclude a positive resolution between Eqs. (1) and (2) as the best description of the dynamics of plastic flow in sapphire. Of significance, however, is that in the temperature range from 1100° to 1700°C the value of H is approximately the same for the various

† $\tau^* = \tau - \tau_\mu$, where τ is the applied shear stress and τ_μ is the long range internal stress. (Refs. 20, 21) On the basis of data in Refs. 7, 8 and 17, $\tau_\mu < 0.3 \text{ Kg/mm}^2 \approx 0$ for annealed crystals and is thus $\approx \Sigma\theta\gamma$ for deformed crystals where θ is the work hardening coefficient given by the slope of the stress-strain curve, and γ is the shear strain.

Table 1. The Values of the Constants A, n, and H in the Equation $\dot{\gamma} = (A/T)[(\tau^*)^n \exp-(H/RT)]$ Derived from Data in the Literature

| Phenomenon | Ref. | $^{\circ}\text{K}/(\text{Kg}/\text{mm}^2)^n$ | n | H Kcal/mole |
|-------------------------------------|------|--|------|--------------------------|
| Internal Friction 1350 - 1850°C | 34 | | | 80 - 140 |
| Proportional Limit 1100 - 1500°C | 17 | 3.61×10^{11} Avg | 3.1 | 104.3 Avg |
| Upper Yield Stress 1200 - 1500°C | 17 | 6.31×10^{11} Avg | 3.8 | 109.5 Avg |
| 1300 - 1750°C | 8 | | 3.4 | $100.4 \pm 12^{\dagger}$ |
| Lower Yield Stress 1200 - 1500°C | 17 | 7.82×10^{11} Avg | 4.2 | 115.0 Avg |
| 1300 - 1750°C | 8 | | 4.5 | $116.8 \pm 9^{\dagger}$ |
| Flow-Creep 1000 - 1200°C | 18 | | ~6.0 | 85 |
| 1200 - 1500°C | 17 | | 5.0 | 110 |
| 1500 - 1900°C | 19 | | 4.5 | 175 - 195 |

[†]Kronberg (Ref. 8) reported values of 95 ± 5 and 85 ± 5 Kcal/mole respectively for the upper and lower yield stresses. The values reported here were derived by the author from Kronberg's data.

yielding (proportional limit, upper yield stress, and lower yield stress) and flow (flow stress, creep) phenomena. Also, Conrad, et al (Ref. 17), found that the values of H for compression were the same as those in tension. This all indicates that the same dislocation mechanism is rate-controlling during flow following the lower yield stress as for yielding, similar to the behavior of the BCC metals (Refs. 22, 23).

A plot of the activation energy obtained using Eq. (1) versus temperature is given in Fig. 10. It is here seen that there appears to be two distinct temperature regions. Below 1500°C the value of H ranges between 80 and 120 Kcal/mole, while above 1500°C it ranges from about 100 to 200 Kcal/mole, there being a strong tendency for the higher values to occur at the higher temperatures. It is noteworthy that Oishi and Kingery (Ref. 24) found that the activation energy for the diffusion of oxygen in sapphire also was higher at temperatures above about 1600°C as compared to that below this temperature, the limits being 58 and 152 Kcal/mole. These latter authors suggested that the high temperature activation energy represented intrinsic diffusion, i. e., the formation of Schottky defects as well as ion mobility, while the low temperature value represented extrinsic diffusion, i. e., only ion mobility.

Figure 11 gives the variation of the activation energy with temperature obtained using Eq. (2). Again, there appear to be two regions, one below 1500°C where the activation energy is approximately proportional to the temperature, and the other above 1500°C where the activation energy increases rapidly to values of the order of 200 Kcal/mole.

A comparison of the available data on the interrelationship between stress, temperature and strain rate [i. e., the values of the parameters of Eqs. (1) and (2)] with various possible thermally activated dislocation mechanisms leads to either one of two possibilities:

1. The climb of dislocations is the rate-controlling mechanism over the entire temperature range from 900° to 2000°C. The variation in H is then

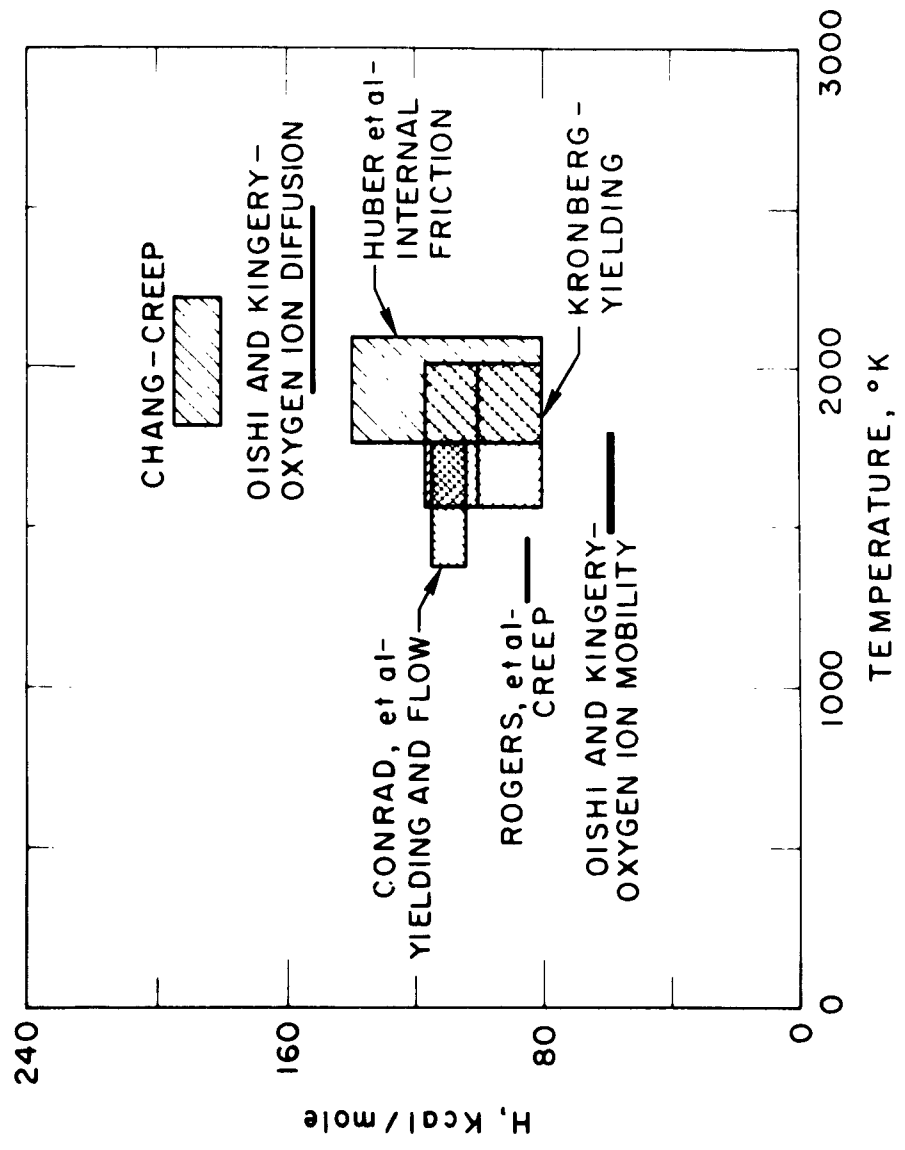


Fig. 10. Activation Energy for Plastic Flow of Sapphire as a Function of Temperature Assuming an Equation of the Form $\dot{\gamma} = A(\tau^n) \exp(-H_0/RT)$.

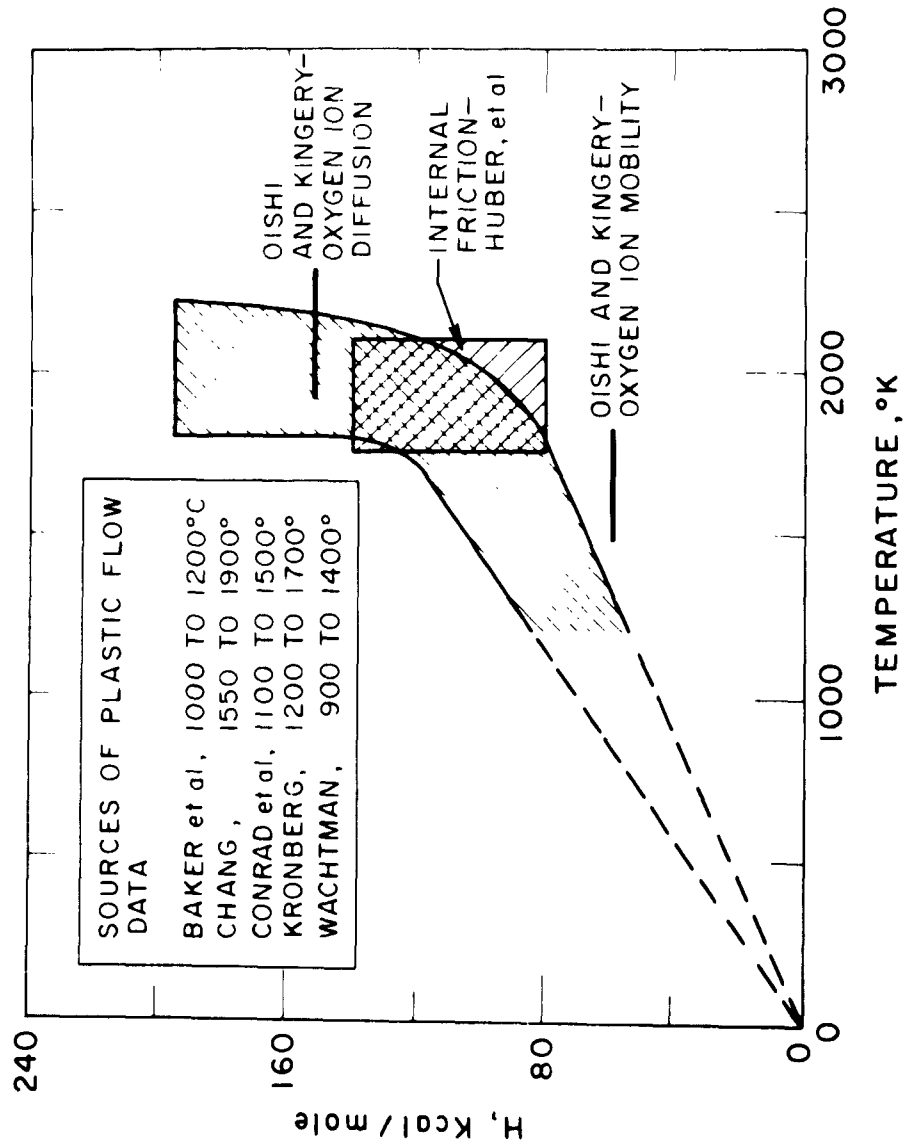


Fig. 11. Activation Energy for Plastic Flow of Sapphire as a Function of Temperature Assuming an Equation of the Form $\dot{\gamma} = \nu \exp[-H(\tau^*)/RT]$

due to the fact that at low temperatures an excess of oxygen ion vacancies are present and, hence, the activation energy for diffusion is more nearly the motion of oxygen ions, while at high temperatures, the activation energy includes the energy to form Schottky defects, as well as the energy for migration. The values of the constants A and n are in reasonable accord with this mechanism.

2. Different dislocation mechanisms operate in the low- and high-temperature regions. A possible mechanism for the low-temperature region is thermally activated overcoming of the Peierls-Nabarro stress, while dislocation climb seems reasonable for the high temperature region. Some support for the Peierls-Nabarro mechanism is provided by the fact that the dislocations in the basal plane are observed to lie along the $\langle 11\bar{2}0 \rangle$ directions (Ref. 14); see Fig. 5. Also, the fact that the activation energy is independent of strain is in accord with the Peierls-Nabarro mechanism.

Additional tests are needed to further resolve the question of the rate-controlling mechanism. Highly desirable would be studies of the effect of temperature and stress on dislocation mobility in sapphire.

D. THE YIELD POINT

The fact that the activation energy for the upper and lower yield stresses is the same as that for subsequent flow suggests that the yield point in sapphire is not due to the tearing of dislocations from a pinning atmosphere, but rather results from a multiplication mechanism associated with the notion of dislocations through the lattice, similar to that postulated by Johnson and Gilman (Ref. 25) for LiF and Conrad (Refs. 22, 26) and Hahn (Ref. 27) for the BCC metals. Additional support for this latter yield-point mechanism is provided by the fact that yield points were also observed following temperature changes or strain-rate changes for strains beyond the lower yield stress (Ref. 7); see, for example, Fig. 9. Furthermore, the strong effect of strain rate on stress (i. e., the low value of n)

observed for sapphire (Table 1) is conducive to such a yield-point mechanism (Ref. 27). However, at present, the mechanism of dislocation multiplication in sapphire is not clear. The double cross-slip mechanism (Refs. 28, 29), applicable to BCC metals, does not appear likely, since cross-slip has not been observed in sapphire at the lower temperatures. One possibility is that Frank-Read type dislocation mills result from the climb of edge components, in the manner discussed by Li (Ref. 30). Also, multiplication may simply occur from Frank-Read sources present in the as-grown crystals.

III. TWINNING

Upon examination of sapphire specimens tested in compression, Stofel and Conrad (Ref. 31) found that many of them exhibited deformation markings or bands, see Fig. 12. Optical and x-ray analyses indicated that these deformation bands were twins of two distinct types, one parallel to the $\{0\bar{1}11\}$ planes and the other parallel to the basal planes. It was established that twinning only occurred at the lower temperatures and higher strain rates. Fig. 13 shows the temperature region in which twinning was observed for compression specimens tested at a strain rate of $5 \times 10^{-5} \text{ sec}^{-1}$. The $(0\bar{1}11)$ twins occurred predominantly at the lowest temperatures and highest strain rates. Basal twinning occurred only in a narrow strain-rate-temperature region bounded by $(0\bar{1}11)$ twinning on the one hand and pure basal glide on the other.

For the orientation range investigated (basal plane oriented 20 deg to 30 deg to the specimen axis), twinning occurred in compression but not in tension. This is expected since, for this orientation, twinning produces a decrease in the total length of the specimen and is thus energetically favorable in compression but not in tension.

$(0\bar{1}11)$ TWINS

(0001) TWINS

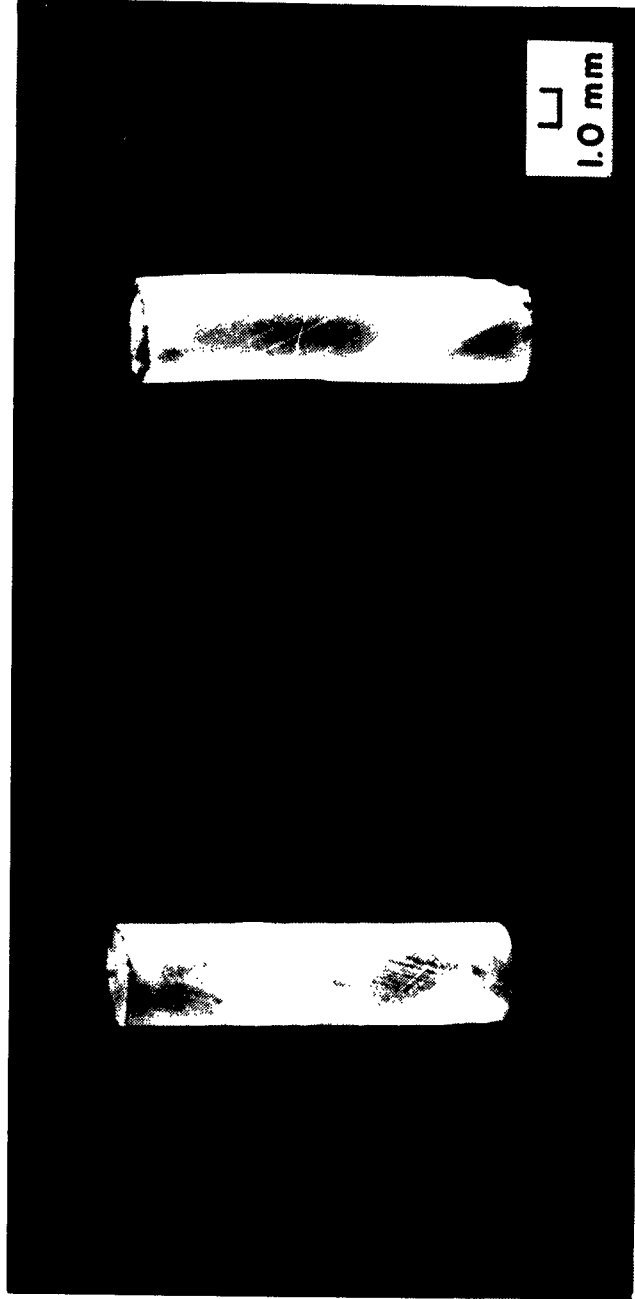


Fig. 12. Twin Bands in Sapphire Compression Specimens [After Stofel and Conrad (Ref. 31)]

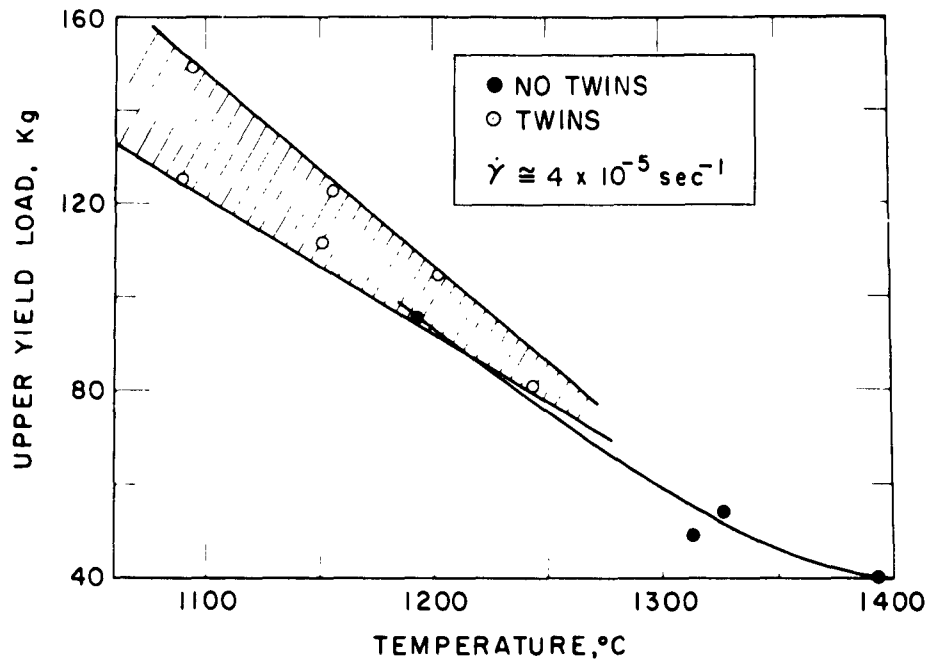


Fig. 13. Effect of Temperature on the Upper Yield Load in Compression and on Twinning [After Conrad, Stone and Janowski (Ref. 17)]

IV. FRACTURE

Fig. 14, taken from a paper by Wachtman and Maxwell (Ref. 32), shows the rupture behavior of sapphire in the temperature range from room temperature to about 1100°C. It is here seen that a decrease in fracture stress occurs between room temperature and 600°C, which is followed by an increase. These authors suggested that microplastic deformation at stress concentrations is responsible for the rise in strength above 600°C.

The fracture of sapphire in tension, compression, and bending was investigated in some detail by Stofel and Conrad (Ref. 31). The most important features of their study will now be covered. They found that the tensile fracture stress of 60 deg sapphire rods in the temperature range from 1100° to 1500°C was dependent only on the amount of previous strain, being independent of the temperature and strain rate; see Fig. 15. The fracture surface was approximately normal to the tensile axis, had its origin where the major axis of the glide ellipse pierced the cylindrical surface of the specimen, and had markings similar to those on the tensile fracture surfaces of glass rods; see Fig. 16. Since the fracture stress increased with strain, and since the origin of the fracture almost invariably occurred where the major axis of the glide ellipse pierced the cylindrical surface of the specimen, these authors concluded that the mechanism of fracture was that originally proposed by Orowan (Ref. 29) to explain how subcritical-size cracks may propagate by interaction with slip dislocations. This mechanism is shown in Fig. 17. The stress field associated with a properly oriented edge dislocation lying near the tip of a crack will add an increment of tensile stress to the stress concentration due to the externally applied force. If the dislocation is close enough to the tip of the crack, the combined tensile stress at the crack tip can be large enough to cause the crack to propagate to the dislocation core. The crack will not propagate beyond the dislocation, however, because the localized stress due to the

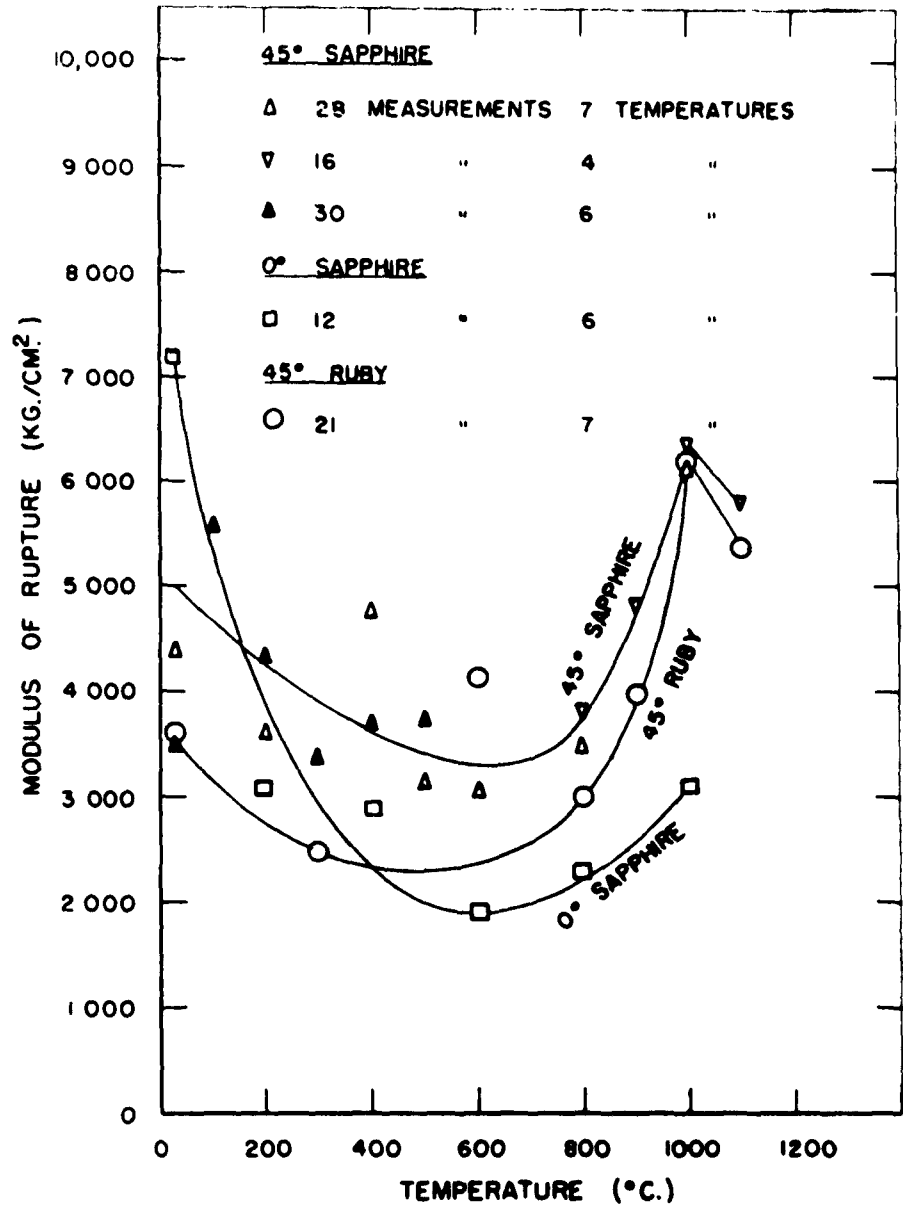


Fig. 14. Effect of Temperature on the Modulus of Rupture of Sapphire and Ruby. [After Wachtman and Maxwell (Ref. 32)]

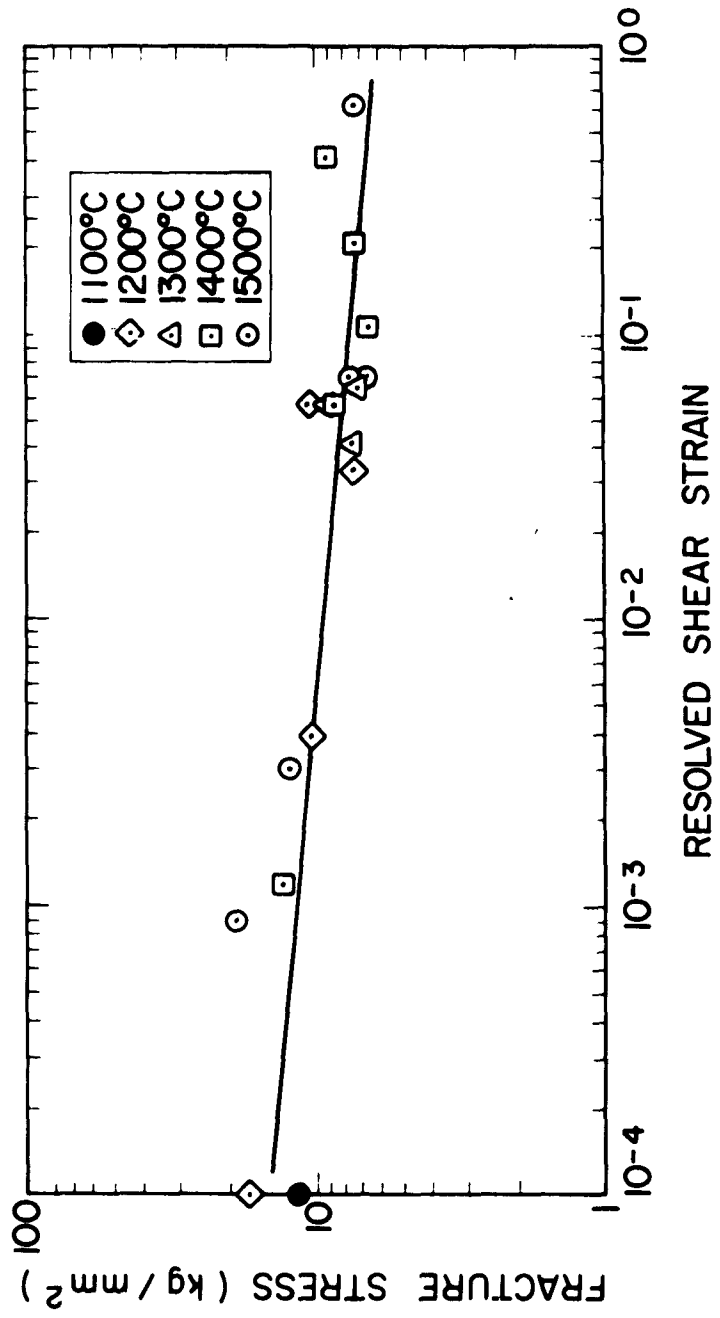


Fig. 15. Variation of the Fracture Stress in Tension with Strain at Fracture. [After Stofel and Conrad (Ref. 31)]

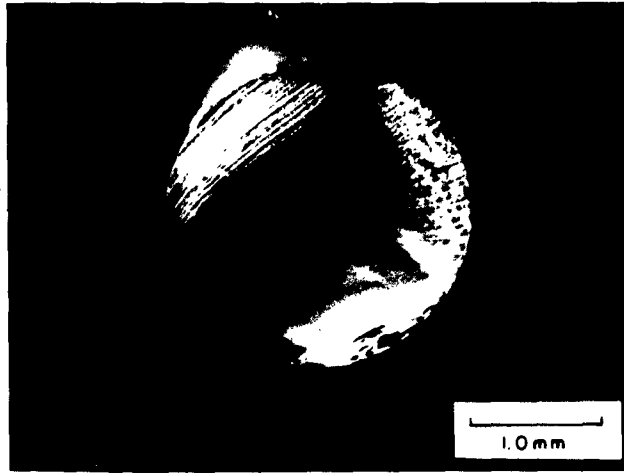


Fig. 16. (a) Typical Fracture Surface Produced During Tensile Testing of a 60 deg Sapphire Rod. Fracture Origin is at Bottom.

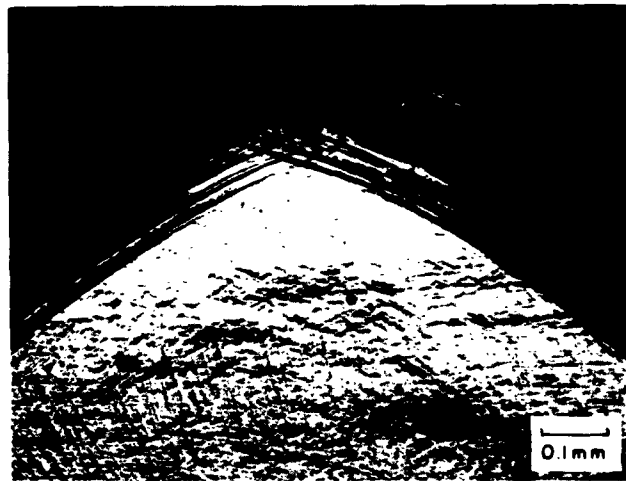


Fig. 16. (b) Enlarged View of Transition from Mirror Area to Wallner Lines on Fracture Surface of Above Figure. [After Stofel and Conrad (Ref. 31)]

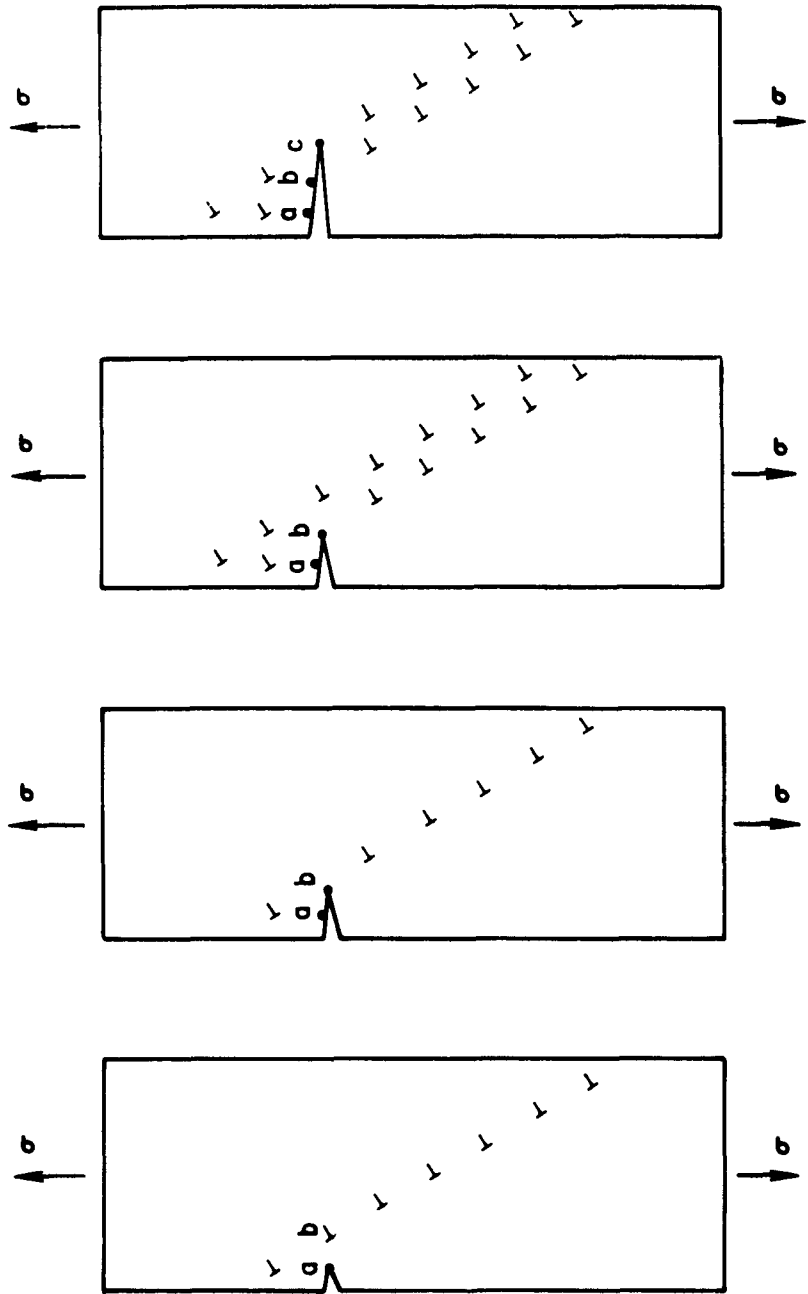


Fig. 17. Orowan's Model of Crack Growth Induced by Plastic Flow. Crack Front Moves from a to c as Plastic Strain Increases. [After Stofel and Conrad (Ref. 31)]

dislocation will be relieved when the crack reaches the dislocation core. Further crack propagation requires plastic flow to bring another edge dislocation near the crack tip. When this process is repeated a sufficient number of times, the crack can grow in incremental steps until it reaches the critical size required for catastrophic propagation by the Griffith mechanism for the particular value of applied stress.

The following relationship between the fracture stress σ_F and plastic strain γ was derived on the basis of the above fracture model:

$$\sigma_F^2 = \frac{1/2 E\rho}{C_0 + C(\gamma)} \quad (3)$$

which gives, upon rearranging

$$1/\sigma_F^2 = \frac{2}{E\rho} [C_0 + C(\gamma)] \quad (3a)$$

where E is Young's modulus, ρ is the surface energy, C_0 is the initial crack length and $C(\gamma)$ is the increase in crack depth as a function of plastic strain. A plot of $1/\sigma_F^2$ vs γ gives some idea as to the manner in which the crack length increases with strain. Such a plot is found in Fig. 18, where it is seen that there is an approximately linear relationship between crack growth and strain up to about 8-percent strain, after which there does not appear to be any further influence of strain. Using values of $E = 30 \times 10^3 \text{ Kg/mm}^2$ and $\rho = 2000 \text{ ergs/cm}^2$ one obtains $C_0 = 10\mu$ from the intercept on the ordinate, which is reasonable.

In bending, 60 deg specimens failed in the manner described above for tension, i. e., with a conchoidal fracture surface similar to that in glass. However, the fracture surface of 0 deg rods (i. e., rod axis parallel to the c -axis) which had failed in bending followed $(10\bar{1}1)$ planes over most of the

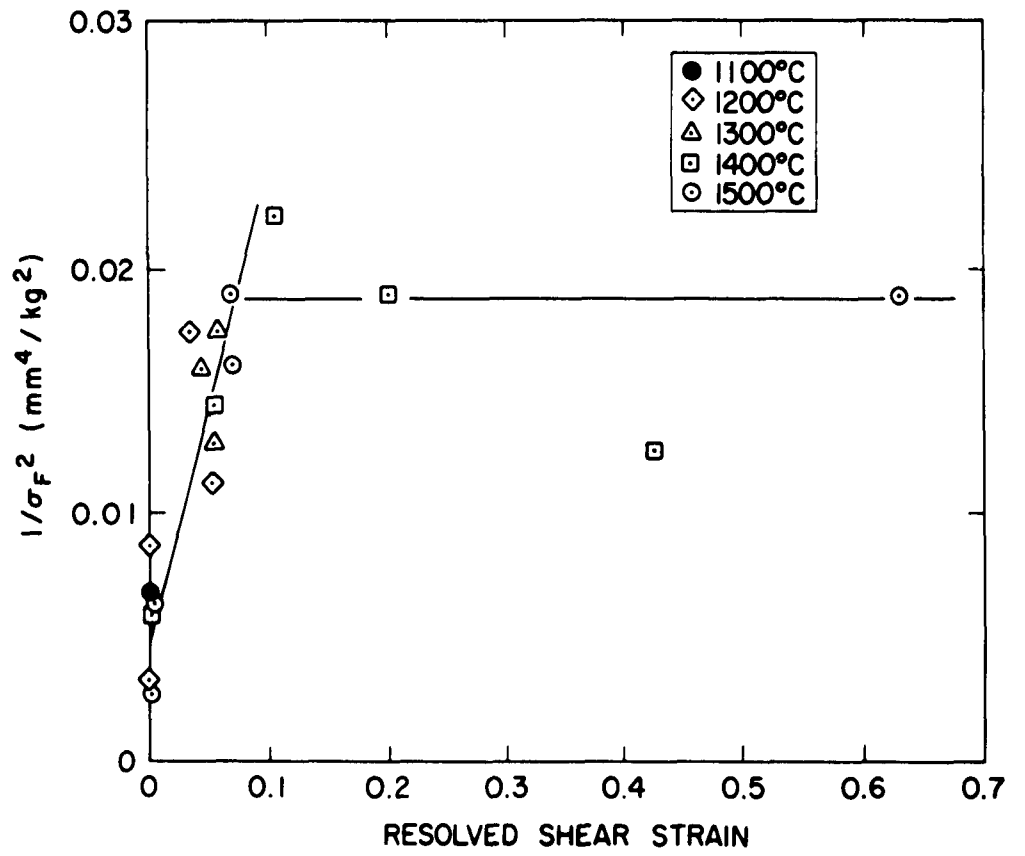


Fig. 18. Reciprocal of Fracture Tensile Stress Squared as a Function of Shear Strain. [After Stofel and Conrad (31)]

surface with the remainder being conchoidal. Optical and x-ray analysis failed to reveal any twins near the fracture surfaces. No explanation can be given at this time for this difference in behavior between the two orientations. However, Laue x-ray spots of the zero-oriented rods were more diffuse than the spots of the 60 deg rods, suggesting a greater defect structure in the former.

Specimens tested in compression failed in several different ways. For small strain rates (10^{-5} sec^{-1}) and high temperatures ($>1400^\circ\text{C}$) the specimens deformed plastically to large shear strains (>25 percent) without fracturing. Specimens tested at high strain rates ($>10^{-3} \text{ sec}^{-1}$) or low temperatures (1100°C) deformed plastically only a small amount prior to failing by the simultaneous occurrence of a large number of fractures approximately parallel to the axis of compression, reducing the specimen to many small splinters. This was probably due to radially directed forces, which resulted from the lack of lubrication between the specimen ends and the compression platens. Specimens tested at intermediate strain rates and temperatures deformed plastically before fracturing into a few pieces, with the fractures again running approximately parallel to the compressive axis. Many of these specimens contained the (0001) and (0 $\bar{1}$ 11) twins mentioned above. Many of the fracture surfaces followed these twinning planes (but not all), suggesting that the twin band interfaces are weaker than the rest of the crystal.

V. SUMMARY

In the following paragraphs our knowledge on the mechanical behavior of sapphire is summarized:

Sapphire deforms plastically above about 900°C , however, the stress for yielding and the amount of strain before fracture is strongly dependent on the strain rate.

The most common mode of deformation of sapphire is by basal slip in the $\langle 11\bar{2}0 \rangle$ direction. However, under certain conditions (especially at temperatures above 1600°C) slip can occur on the prism planes in the $\langle 11\bar{2}0 \rangle$ direction. Also, twinning may occur at low temperatures and high strain rates for favorable conditions.

Yielding in sapphire can occur discontinuously with the appearance of upper and lower yield points, whose difference increases with increase in strain rate and decrease in temperature. This yield point is better described in terms of a dislocation multiplication mechanism based on the motion of dislocations through the lattice than the thermally assisted tearing of dislocations from an impurity (or other defect) atmosphere.

The dynamics of yielding and flow can be expressed by either of two thermally activated equations. In one, the effect of stress is principally on the pre-exponential frequency factor; in the other its effect is principally on the activation energy for plastic flow. The activation energy derived from these equations appears to have two limiting values. At temperatures below 1200°C it is approximately 80 Kcal/mole, while above 1800°C it is about 180 Kcal/mole. In the intermediate temperature range the activation energy varies between these two limits. These activation energy limits are only roughly in accord with those of oxygen ion mobility and oxygen ion diffusion, respectively.

The activation energy values suggest either that (1) dislocation climb is rate-controlling over the entire temperature range, or that (2) overcoming the Peierls-Nabarro stress is rate-controlling at low temperatures ($<1500^\circ\text{C}$) and dislocation climb at high temperatures.

Upon compressing sapphire rods, twinning occurs on the (0001) and (0 $\bar{1}$ 11) planes. These twins occur most readily at the lower temperatures and higher strain rates.

The fracture of 60 deg sapphire rods in tension, bending, and compression generally occurs on a plane approximately normal to the tensile

stress, and the fracture surface is conchoidal. The fracture stress decreases with increase in previous plastic strain, independent of temperature and strain rate. The mechanism of failure seems to be the interaction of edge dislocations with pre-existing surface cracks. When twinning occurs, the fracture surface tends to follow the twin interface, suggesting that this is weaker than the untwinned crystal.

Zero-degree oriented crystals stressed in bending fracture along $(0\bar{1}11)$ planes, suggestive of cleavage fracture.

REFERENCES

1. M. L. Kronberg, Acta Met. 5, 507 (1957).
2. J. F. Nye, Acta Met. 1, 153 (1953).
3. J. B. Wachtman and L. H. Maxwell, J. Am. Ceram. Soc. 37, 291 (1954).
4. J. B. Wachtman and L. H. Maxwell, J. Am. Ceram. Soc. 40, 377 (1957).
5. M. L. Kronberg, Science 122, 599 (1955).
6. R. Scheuplein and P. Gibbs, J. Am. Ceram. Soc. 43, 458 (1960).
7. H. Conrad, "Yielding and Flow of Sapphire (α - Al_2O_3 Crystals)" Tech. Report No. NAA-SR-6543 Atomics International Div., North American Aviation Inc., Canoga Park, California (1961).
8. M. L. Kronberg, J. Am. Ceram. Soc. 45, 274 (1962).
9. J. B. Wachtman, Creep and Recovery (ASM, Cleveland, 1957) p. 344.
10. J. B. Wachtman and L. H. Maxwell, reported by Scheuplein and Gibbs in Ref. 4.
11. W. J. Alford and D. L. Stephens, J. Am. Ceram. Soc. 46, 193 (1963).
12. K. Janowski and H. Conrad, "Dislocations in Ruby Laser Crystals," Report No. TDR-169(3240-01)TN-2. Aerospace Corporation, El Segundo, California (July 29, 1963), to be published in Trans. AIME.
13. H. Palmour III and W. W. Kriegel, "Brittleness in Ceramics I - Dislocations in Single Crystal Sapphire Revealed by Thermal Etching," Engineering Study Report, Contract No. DA-36-034-ORD-2645, North Carolina State College (January 1961).
14. H. E. Bond and K. B. Harvey, J. Appl. Phys. 34, 440 (1963).
15. T. A. Voruz, R. P. Jewett, and O. E. Accountius, J. Am. Ceram. Soc. 46, 459 (1963).

REFERENCES (Continued)

16. J. B. Wachtman, paper at Brittle Fracture Meeting, Illinois Institute of Technology Research Institute, Chicago, Illinois (Feb. 24, 1964).
17. H. Conrad, G. Stone and K. Janowski, submitted to Trans. AIME.
18. W. G. Rogers, G. S. Baker and P. Gibbs, Mechanical Properties of Engineering Ceramics, (Interscience, New York, 1961) p. 303.
19. R. Chang, J. Appl. Phys. 31 484 (1960).
20. H. Conrad and H. Wiedersich, Acta Met. 8, 128 (1960).
21. H. Conrad, "Thermally Activated Deformation of Metals," to be published in AIME J. of Met.
22. H. Conrad, J. Iron and Steel Inst. 198, 364 (1961).
23. H. Conrad and W. Hayes, Trans. Am. Soc. Metals 56, 249 (1963).
24. Y. Oishi and W. D. Kingery, J. Chem. Phys. 35, 480 (1960).
25. W. G. Johnson and J. J. Gilman, J. Appl. Phys. 30, 129 (1959).
26. H. Conrad, Iron and Its Dilute Solid Solutions (Interscience, New York, 1963) p. 315.
27. G. Hahn, Acta Met. 10, 727 (1962).
28. J. S. Koehler, Phys. Rev. 86, 52 (1952).
29. E. Orowan, Dislocations in Metals (AIME, New York, 1954) p. 69.
30. J. C. M. Li, J. Appl. Phys. 32, 593 (1961).
31. E. Stofel and H. Conrad, Trans AIME 227, 1053 (1963).
32. J. B. Wachtman and L. H. Maxwell, J. Am. Ceram. Soc. 42, 432 (1959).
33. E. Orowan, Dislocations in Metals (AIME publication, New York, 1954) p. 191.
34. R. J. Huber, G. S. Baker, and P. Gibbs, "Internal Friction in Aluminum Oxide Single Crystals", Tech. Rept. XIV, Contract No. N-ONR-1288(03), Univ. of Utah, Nov. 1, 1960, J. Appl. Phys. 32, 2573 (1961).